

Original Article

Clinical findings and imaging features of 67 nasopharyngeal carcinoma patients with postradiation nasopharyngeal necrosis

Ming-Yuan Chen^{1,2}, Hai-Qiang Mai^{1,2}, Rui Sun^{1,2}, Xiang Guo^{1,2}, Chong Zhao^{1,3}, Ming-Huang Hong^{1,2} and Yi-Jun Hua^{1,2}

Abstract

Postradiation nasopharyngeal necrosis is an important late effect of radiotherapy that affects prognosis in patients with nasopharyngeal carcinoma. In the present study, we reviewed the clinical and imaging features of 67 patients with pathologically diagnosed postradiation nasopharyngeal necrosis who were treated at Sun Yat-sen University Cancer Center between June 2006 and January 2010. Their clinical manifestations, endoscopic findings, and imaging features were analyzed. Early nasopharyngeal necrosis was limited to a local site in the nasopharyngeal region, and the tissue defect was not obvious, whereas deep parapharyngeal ulcer or signs of osteoradionecrosis in the basilar region was observed in serious cases. Those with osteoradionecrosis and/or exposed carotid artery had a high mortality. In conclusion, Postradiation nasopharyngeal necrosis has characteristic magnetic resonance imaging appearances, which associate well with clinical findings, but pathologic examination is essential to make the diagnosis.

Key words Nasopharyngeal carcinoma, radiation, necrosis, magnetic resonance imaging, osteoradionecrosis

Nasopharyngeal carcinoma (NPC) is a common malignancy in Southeast Asia^[1]. Radiotherapy is an effective treatment for NPC. However, radiation may cause both acute effects, which occur during radiation and in the immediate weeks and months following treatment, and late effects, which develop gradually over several months or years, on the bones and soft tissues surrounding the neck and nasopharynx^[2]. As the number of NPC survivors who have undergone radiation increases, so too does the incidence of postradiation complications, including postradiation nasopharyngeal necrosis.

Postradiation nasopharyngeal necrosis is necrosis of the surrounding and affiliated tissues of the nasopharynx, such as the mucosa, musculus longus capitis, parapharyngeal tissues, and skull base, that have been exposed to radiation months or years ago^[3]. Postradiation nasopharyngeal necrosis becomes life threatening

when the carotid sheath is involved, especially when internal carotid artery is eroded. It is important for clinical doctors to realize this problem in order to cope with this severe clinical situation.

In this study, we aimed to define the clinical features of postradiation nasopharyngeal necrosis through reviewing the clinical and imaging features of 67 NPC patients with postradiation nasopharyngeal necrosis.

Patients and Methods

Patients

Between June 2006 and January 2010, 67 patients (11 women and 56 men) with pathologically diagnosed nasopharyngeal necrosis were treated at the Department of Nasopharyngeal Carcinoma, Sun Yat-sen University Cancer Center, Guangzhou, China. Four patients presented with both necrosis and tumor recurrence and were not included in this study.

Of the 67 patients, 40 patients underwent one circle of radiotherapy, including 28 treated with two-dimensional conventional radiotherapy (2D-CRT) and 12 with intensity-modulated radiotherapy (IMRT), and 27 patients underwent two courses of radiotherapy due to recurrent tumors. Of the 27 patients with recurrent tumors, 3 underwent two courses of CRT, 5 underwent two courses of IMRT, 18 underwent one course of CRT followed by a course of IMRT, and 1

Authors' Affiliations: ¹State Key Laboratory of Oncology in South China, Guangzhou, Guangdong 510060, P. R. China; ²Department of Nasopharyngeal Carcinoma; ³Department of Radiotherapy, Sun Yat-sen University Cancer Center, Guangzhou, Guangdong 510060, P. R. China.

Corresponding Author: Yi-Jun Hua, Department of Nasopharyngeal Carcinoma, Sun Yat-sen University Cancer Center, 651 Dongfeng Road East, Guangzhou, Guangdong 510060, P. R. China. Tel: +86-20-87343379; Fax: +86-20-87343392; Email: huayj@sysucc.org.cn

doi: 10.5732/cjc.012.10252

underwent one course of CRT followed by a course of X knife (**Table 1**).

Nasopharyngeal necrosis was diagnosed on the basis of characteristics, clinical manifestations, magnetic resonance imaging (MRI) features, endoscopic findings, and pathologic findings. Repetitive histologic examination of nasopharyngeal specimens showed features of tissue necrosis. All patients were evaluated clinically at the time of diagnosis and follow-up MRI study.

All patients were examined with MRI every three months during the first year after radiotherapy. Follow-up information was obtained from the patients' medical records and by telephone calls radiotherapy to the patients. The follow-up period of the current study was defined from the end of radiotherapy to the last follow-up day, April 6, 2011.

MRI

All patients underwent MRI with a 1.5-T system (Signa, General Electric, CV/i; General Electric Healthcare, Chalfont St. Giles, United Kingdom). The area from the suprasellar cistern to the inferior margin

of the sternal end of clavicle was examined with a head-and-neck combined coil. T1-weighted fast spin-echo images on the axial, coronal, and sagittal planes (repetition time of 500–600 ms and echo time of 10–20 ms), and T2-weighted fast spin echo MRI images on the axial plane (repetition time of 4,000–6,000 ms and echo time of 95–110 ms) were obtained before injection of contrast reagent. After intravenous gadolinium diethylene triaminepenta acetate (Gd-DTPA) injection at a dose of 0.1 mmol/kg of body weight, T1-weighted spin-echo axial and sagittal sequences as well as T1-weighted spin-echo fat-suppressed coronal sequences were performed sequentially, with parameters similar to those used before Gd-DTPA injection. Section thickness was 5 mm with a 1-mm interslice gap for the axial plane and 6 mm with a 1-mm interslice gap for the coronal and sagittal planes. The MRI images were assessed independently by two radiologists, and the final interpretation of the results was reached by consensus between the two radiologists.

Treatment of postradiation nasopharyngeal necrosis

Debridement guided by nasal endoscopy and excision of the

Table 1. Characteristics of 67 patients with nasopharyngeal carcinoma who had postradiation nasopharyngeal necrosis

Characteristic	No. of patients (%)
Sex	
Male	56 (83.6)
Female	11 (16.4)
Age (years)	
Range	29–74
Median	53
Circles of radiation and its techniques	
Single course	40 (59.7)
CRT	28
IMRT	12
Two courses	27 (40.3)
CRT-CRT	3
CRT-IMRT	18
IMRT-IMRT	5
CRT (X knife)-IMRT	1
Interval ^a (months)	
Range	2–14
Median	6
Lesion area	
Extensive lesion area	49 (73.1)
Local lesion areas	18 (26.9)
Osteoradionecrosis	38 (56.7)
Carotid artery exposure	33 (49.3)
Treatment outcome	
Alive	39 (58.2)
Died	28 (41.8)

^aThe time from the completion of radiotherapy to the diagnosis of post-radiation nasopharyngeal necrosis. CRT, conventional radiotherapy; IMRT, intensit-modulated radiotherapy.

radiation-induced necrotic tissues were performed every one or two weeks for all 67 patients until they were considered cured or their clinical symptoms, such as foul odor, headache, and hemorrhage, were alleviated. Conservative treatment included daily nasopharyngeal rinsing with 2% aqueous hydrogen dioxide (5–10 mL per rinse) or saline (50–100 mL per rinse) along with antibiotic therapy (metronidazole or ornidazole) guided by culture results. Intravenous nutrition and systematic antibiotic therapy were also performed if indicated and necessary.

Statistical analyses

SPSS software (SPSS Inc. version 16.0, Chicago, IL) was used to analyze the data. Chi-square test was used to compare the difference between groups. A *P* value of < 0.05 was considered statistically significant.

Results

Clinical features and outcomes of patients with postradiation nasopharyngeal necrosis

The clinical characteristics of the patients included in this study are summarized in **Table 1**. All 67 patients experienced foul nasal odor and persistent headache. Refractory headache was noted in patients with osteoradionecrosis. Fifty patients also experienced repeated nasal hemorrhage or bloody nasal mucus. Those symptoms

occurred at 2 to 14 months (median, 6 months) after the completion of radiotherapy. All necrotic foci arose within the field of radiation.

At the end of the follow-up period, 39 patients were alive, including 9 deemed cured, whereas 18 patients died due to massive nasopharyngeal hemorrhage and 10 patients died due to prostration.

Two patients appeared lethal intracranial infection due to osteoradionecrosis, sequential cerebrospinal fluid rhinorrhea, and intracranial infection.

MRI features of patients with postradiation nasopharyngeal necrosis

MRI revealed different abnormalities consistent with radiation injury among patients with postradiation nasopharyngeal necrosis. Eighteen patients (26.9%) presented with local erosion, which did not exceed the midline of the nasopharynx (**Figure 1**), and 49 patients (73.1%) presented with extensive erosion, which exceeded the midline of the nasopharynx. Furthermore, 33 patients (49.3%) showed internal carotid artery exposure (**Figure 2**), and 38 patients (56.7%) presented with osteoradionecrosis (**Figure 3**).

Correlation between MRI and clinical outcome

Twenty-three of the 49 patients (46.9%) who presented with extensive lesion areas died, whereas only 5 of the 18 patients (27.8%) with local lesion areas died ($P < 0.01$). Of the 38 patients with osteoradionecrosis, 25 (65.8%) died, whereas only 3 of the

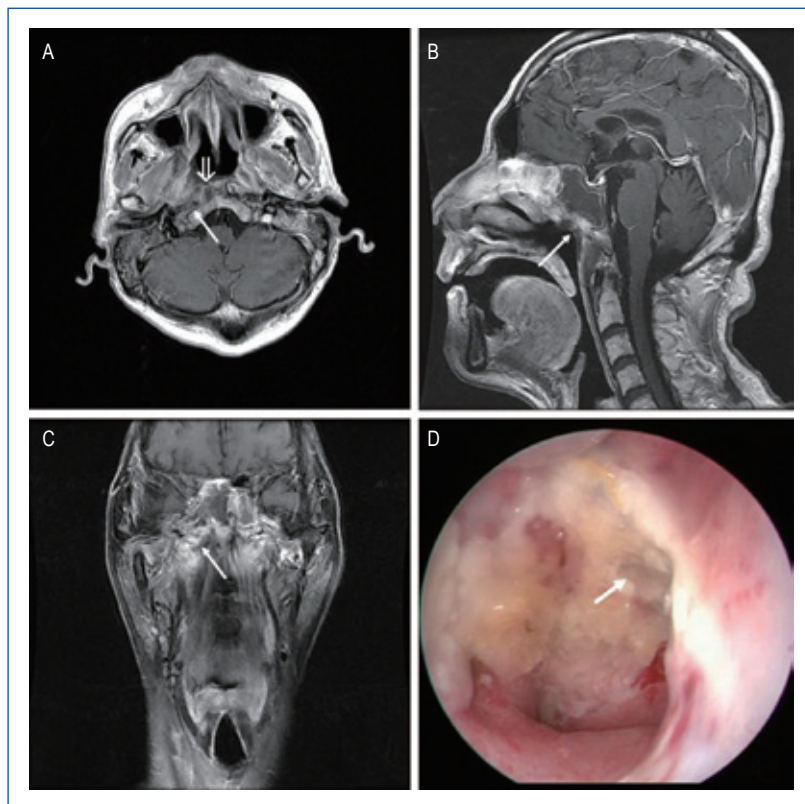


Figure 1. Magnetic resonance imaging (MRI) and endoscopic findings of a postradiation nasopharyngeal necrosis with local erosion. MRI images were obtained on a 55-year-old man who underwent intensity-modulated radiotherapy (IMRT) due to recurrent tumor 8 years after the first course of conventional radiotherapy (CRT). A, transverse, contrast-enhanced, T1-weighted MRI image showing the nonenhanced soft tissues mixed with tiny air bubbles in right-sided nasopharyngeal lateral recess (arrow). The nasopharyngeal mucosa line is discontinuous (open arrow). B, sagittal, contrast-enhanced, T1-weighted MRI image showing the necrotic mass with extension into the roof of nasopharynx. There is a defect in the roof (arrow). C, coronal, T1-weighted image shows the defect in the right wall is extended to the right parapharyngeal space (arrow). D, necrosis is located in the right roof of the nasopharyngeal cavity, and there is a defect in the roof (arrow; observed under telescope 0°).

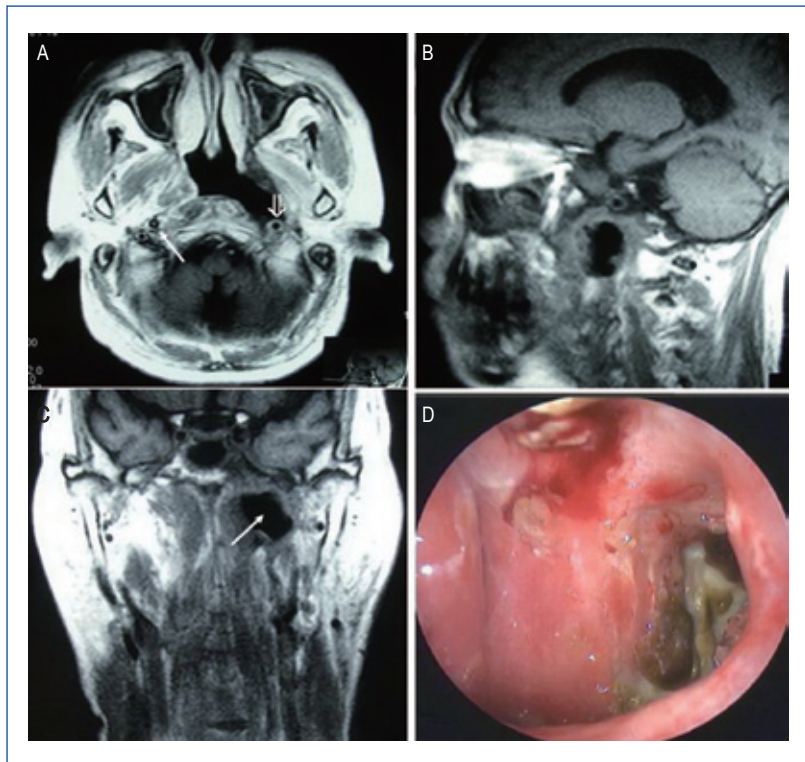


Figure 2. MRI and endoscopic findings of a postradiation nasopharyngeal necrosis with erosion and carotid exposure.

MRI images were obtained on a 56-year-old man who underwent CRT after the second course of radiotherapy. The man died of massive bleeding 3 months after the diagnosis of postradiation nasopharyngeal necrosis. A, transverse T1-weighted image showing nasopharyngeal necrosis is mainly located in the left wall of nasopharyngeal cavity. There is a defect in the left parapharyngeal space, and the internal carotid artery is involved (open arrow). Note the normal right carotid artery for comparison (arrow). B, sagittal T1-weighted image showing a defect in the posterior wall and the discontinuity of the posterior soft tissue. C, coronal T1-weighted image showing the defect in the left wall is extended to the left parapharyngeal space (arrow). D, necrosis is located in the left wall of the nasopharyngeal cavity, and the cavity is covered with secretion and necrotic tissue (observed under telescope 0°).

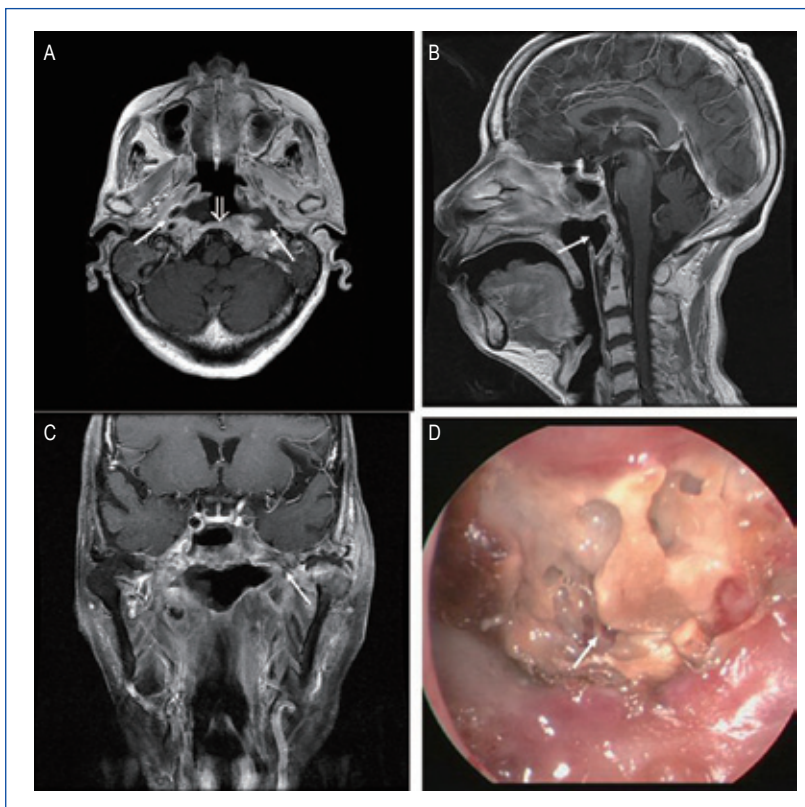


Figure 3. MRI and endoscopic findings of a postradiation nasopharyngeal necrosis with extension erosion and osteoradionecrosis.

MRI images were obtained on a 74-year-old woman who underwent CRT. A, transverse T1-weighted image shows that the destruction of the bone was extensive and that the lesions involved the clivus (open arrow) and bilateral parapharyngeal space (arrows). B, sagittal T1-weighted image showing a hollow defect in the posterior wall (arrows). C, coronal T1-weighted image shows that the necrosis is extensive and small air bubbles are present (arrow). D, the necrosis is located in the posterior wall of the nasopharyngeal cavity and the sequestra can be seen within the necrotic bones (arrow; observed under telescope 0°).

29 patients (10.3%) without osteoradionecrosis died ($P < 0.01$). Moreover, 24 of the 33 patients (72.7%) with carotid artery exposure died, whereas only 4 of 34 patients (11.8%) without exposure died ($P < 0.01$). Patients with extensive lesion areas, osteoradionecrosis, or carotid artery exposure had a high mortality (**Table 2**).

Discussion

This study was conducted to evaluate the MRI characteristics and clinical features of postradiation nasopharyngeal necrosis in NPC. We found that postradiation nasopharyngeal necrosis has characteristic MRI appearances, which associate well with the clinical features.

NPC is a common malignancy in Southeast Asia, especially in southern China, and the incidence among Cantonese is still the highest reported in the world despite an appreciable decrease over time^[4]. At our cancer center, more than 2,000 patients are diagnosed with NPC each year. At present, radiotherapy is the mainstay of treatment for NPC. However, radical radiation can both significantly improve survival and cause consequential late effects. Of these late effects, postradiation nasopharyngeal necrosis results in poor quality of life and poor prognosis in our clinical observation.

MRI has been found to be more sensitive than computed tomography for the detection of radiation-induced temporal lobe necrosis, osteoradionecrosis, and necrosis of soft tissue^[5-8]. Pruzincova *et al.*^[9] reported that advanced MRI techniques allow for the assessment of metabolism and physiology and may increase specificity for therapy-induced changes. The present study revealed several MRI features. Almost every case of NPC demonstrated no enhancement on MRI images. Necrotic areas or non-enhanced regions were common, but focal tissue necrosis was a unique event after radiation therapy. MRI scans also show defects in the nasopharyngeal wall. When pathologic changes deteriorate, MRI shows obvious defects in the nasopharyngeal wall along with tiny air bubbles in the nasopharyngeal lateral recess. If osteoradionecrosis appears, the bone and internal carotid artery lose soft tissue

coverage and are exposed to the air cavity. In our cohort of patients, the destruction of the bone was extensive and symmetric or localized. Lesions involved the whole skull base with the sphenoid bone (most frequently) or with the clivus or internal carotid canal (less frequently), and sequestra can also be seen within or surrounding necrotic bones even small air bubbles were present in the soft tissue adjacent to the necrotic bone. In our study, MRI revealed 18 patients (26.9%) with local erosion and 49 patients (73.1%) with extensive erosion, 38 patients (56.7%) with osteoradionecrosis, and 33 patients (49.3%) with internal carotid artery exposure. We expect that patients with necrosis and recurrent tumor would also show similar MRI features, but those cases would be accompanied by enhanced tissue, a crucial factor to differentiate recurrent tumor from necrosis.

According to the literature, necrosis can be described as a process with three stages^[10], each with characteristic features on MRI. In the early stage, pathologic changes occur in the nasopharyngeal mucosa, including local mucosa denaturalization—the primary endoscopic finding. Also, in this stage, the nasopharyngeal mucosa line is discontinuous. Accordingly, patients with early-stage necrosis experience mild headache and faint foul nasal odor. In the second stage, pathologic changes occur in the soft tissue, including the nasopharyngeal mucosa, muscle, and tendon. Thus, MRI shows nasopharyngeal necrosis that is mainly located in the wall of nasopharyngeal cavity. Transverse contrast-enhanced, T1-weighted MRI images show the non-enhanced soft tissues mixed with tiny air bubbles in the nasopharyngeal recess. Defects in the parapharyngeal space and involvement of the internal carotid artery can also be observed. The severe stage, third in the process, corresponds to skull base osteoradionecrosis, which causes refractory headache. MRI shows lesions involving the clivus, atlas, and even cervical vertebrae. Although MRI findings are diagnosis-specific, pathologic evidence is still necessary to support the diagnosis.

Prognosis in patients with nasopharyngeal necrosis is generally poor^[10]. Hemorrhage, a fatal event, is closely associated with radiation-induced nasopharyngeal necrosis. Weakening of the wall of

Table 2. Association between magnetic resonance imaging and clinical outcome

MRI feature	Clinical outcome		P
	Survival	Died	
Lesion			0.005
Extensive	26	23	
Local	13	5	
Osteoradionecrosis			<0.001
Yes	13	25	
No	26	3	
Carotid artery exposure			<0.001
Yes	9	24	
No	30	4	

postirradiated vessels may result in dissection or rupture and produce a pseudoaneurysm^[11,12]. Without immediate treatment in a hospital, rupture can be fatal because of the anatomy of the nasopharynx. The parapharyngeal space is a loose network of fibrofatty tissue between the pharyngeal and pterygoid musculature in the posterolateral part of the nasopharynx, where necrosis usually occurs. Without the coverage and protection from this tissue, the injured internal carotid artery is prone to bleed. In our series, 26.9% of the patients died of acute hemorrhage within two years of being diagnosed with nasopharyngeal necrosis.

The exact mechanism of PRNN is unknown. The infection was reported to play an important role in the process of nasopharyngeal necrosis^[13]. Infection of a local nasopharyngeal region may increase the demand of the local tissue for energy, oxygen, and other metabolites, which leading to collagen destruction and cell death^[14]. Hypoxia and radiation factors such as dosage and dose rate also play an important role^[15]. Radiation obliterates the vasa vasorum and causes premature atherosclerosis, adventitial fibrosis, and weakening and necrosis of the arterial wall. The results of many studies about

osteoradionecrosis show that the dosage was highly related with the occurrence of skull base osteoradionecrosis^[11,14-16]. Of the 67 patients studied here, 27 underwent two courses of radiotherapy and 12 underwent IMRT. For patients who received radiotherapy, the accumulating prescribed dose for the nasopharynx was more than 120 Gy. For the patients treated with IMRT, the dose for the nasopharynx was more than 80 Gy. Retrospective view of MRI films shows the consistence of the necrotic area with the area subjected to the highest dose.

In conclusion, postradiation nasopharyngeal necrosis has characteristic MRI appearances, which associate well with the clinical features. Thus, recognition of the MRI features may be helpful. MRI findings are diagnosis-specific and may therefore help the doctor to stage the severity of the necrosis. Nevertheless, the final diagnosis of postradiation nasopharyngeal necrosis should be made with pathologic evidence.

Received: 2012-10-11; revised: 2013-02-04;
accepted: 2013-02-13.

References

- [1] Yu MC, Yuan JM. Epidemiology of nasopharyngeal carcinoma. *Semin Cancer Biol*, 2002,12:421–429.
- [2] Lee AW, Law SC, Ng SH, et al. Retrospective analysis of nasopharyngeal carcinoma treated during 1976–1985: late complications following megavoltage irradiation. *Br J Radiol*, 1992,65:918–928.
- [3] Hua YJ, Chen MY, Hong MH, et al. Short-term efficacy of endoscopy-guided debridement on radiation-related nasopharyngeal necrosis in 20 nasopharyngeal carcinoma patients after radiotherapy. *Ai Zheng*, 2008,27:729–733. [in Chinese]
- [4] Lee AW, Foo W, Mang O, et al. Changing epidemiology of nasopharyngeal carcinoma in Hong Kong over a 20-year period (1980–99): an encouraging reduction in both incidence and mortality. *Int J Cancer*, 2003,103:680–685.
- [5] Chan YL, Leung SF, King AD, et al. Late radiation injury to the temporal lobes: morphologic evaluation at MR imaging. *Radiology*, 1999,213:800–807.
- [6] King AD, Tse GM, Ahuja AT, et al. Necrosis in metastatic neck nodes: diagnostic accuracy of CT, MR imaging, and US. *Radiology*, 2004,230:720–726.
- [7] Wang YX, King AD, Zhou H, et al. Evolution of radiation-induced brain injury: MR imaging-based study. *Radiology*, 2010,254:210–218.
- [8] Malizos KN, Karantanas AH, Varitimidis SE, et al. Osteonecrosis of the femoral head: etiology, imaging and treatment. *Eur J Radiol*, 2007,63:16–28.
- [9] Pruzincova L, Steno J, Srbecky M, et al. MR imaging of late radiation therapy- and chemotherapy-induced injury: a pictorial essay. *Eur Radiol*, 2009,19:2716–2727.
- [10] Hua YJ, Chen MY, Qian CN, et al. Postradiation nasopharyngeal necrosis in the patients with nasopharyngeal carcinoma. *Head Neck*, 2009,31:807–812.
- [11] Chen HC, Lin CJ, Jen YM, et al. Ruptured internal carotid pseudoaneurysm in a nasopharyngeal carcinoma patient with skull base osteoradionecrosis. *Otolaryngol Head Neck Surg*, 2004,130:388–390.
- [12] Chin SC, Jen YM, Chen CY, et al. Necrotic nasopharyngeal mucosa: an ominous MR sign of a carotid artery pseudoaneurysm. *AJNR Am J Neuroradiol*, 2005,26:414–416.
- [13] Hao SP, Chen HC, Wei FC, et al. Systematic management of osteoradionecrosis in the head and neck. *Laryngoscope*, 1999,109:1324–1328.
- [14] Marx RE. Osteoradionecrosis: a new concept of its pathophysiology. *J Oral Maxillofac Surg*, 1983,41:283–288.
- [15] Huang XM, Zheng YQ, Zhang XM, et al. Diagnosis and management of skull base osteoradionecrosis after radiotherapy for nasopharyngeal carcinoma. *Laryngoscope*, 2006,116:1626–1631.
- [16] Auyeung KM, Lui WM, Chow LC, et al. Massive epistaxis related to petrous carotid artery pseudoaneurysm after radiation therapy: emergency treatment with covered stent in two cases. *AJNR Am J Neuroradiol*, 2003,24:1449–1452.